Exploring the pressurized heterogeneous electro-Fenton process and modelling the system

Verónica Poza-Nogueiras[a,b], Ángela Moratalla[b], Marta Pazos[a], Ángeles Sanromán[a], Cristina Sáez[b], Manuel A. Rodrigo[b*]

[a] CINTECX, Universidade de Vigo, Departamento de Enxeñaría Química, Campus Lagoas Marcosende, 36310 Vigo, Spain

[b] Chemical Engineering Department, Facultad de Ciencias y Tecnologías Químicas, University of Castilla-La Mancha, Edificio Enrique Costa Novella, Av. Camilo José Cela 12, 13071 Ciudad Real, Spain

* Corresponding author: Cristina Sáez (cristina.saez@uclm.es)

ABSTRACT

In this research, a bench-scale installation was tested for the heterogeneous electro-Fenton treatment of clofibric acid. The setup consists of a pressurized flow-through electrochemical cell equipped with a catalyst fluidized-bed and aerated with a jet mixer. The novelty of the research is two-fold: the use of the pressurized-jet aerator on an electro-Fenton treatment is tested and it is one of the first studies combining pressure with heterogeneous catalysis in electro-Fenton. Moderate relative pressures, up to 2 bar, were analyzed. Initially, the electrogeneration of hydrogen peroxide was tested, showing that it is remarkably boosted by the application of pressure. Then, the elimination of clofibric acid by means of an electro-Fenton treatment was carried out at 0.12 and 0.25 A, using iron-containing alginate beads as the catalyst. Regardless of the current intensity, the increase from atmospheric pressure to 1 gauge bar boosted the elimination of the pollutant and reduced the specific energy consumption of the electrochemical cell. Specifically, at 0.25 A an abatement higher than 98% was achieved in 8 h at atmospheric pressure while only 1 h was required at 1 bar of gauge pressure. However, a further increase of the pressure to 2 bar did not report a major improvement. Moreover, the effect of pressure on the catalyst was analyzed, concluding that the integrity of the alginate beads was not compromised by pressure. In fact, the iron leaching was very similar at 0, 1 and 2 bar: around 30% after 8 h of treatment. Finally, a mathematical model was developed, using

the experimental data to obtain the necessary fitting parameters, which allowed to understand better the behavior of the bench-scale reaction system.

Keywords heterogeneous catalyst, iron-containing alginate gel beads, pressure, jet aerator, microfluidic flow-through electrochemical reactor, modelling

1. INTRODUCTION

The detection of pharmaceuticals and pesticides in water environments is a widely recognized issue, due to the potential threat they pose to human health and aquatic life [1]. One example of those kind of compounds is clofibric acid. It is a bioactive metabolite of clofibrate, etofibrate and etofyllinclofibrate, pharmaceuticals used for blood lipid regulation [2]. In addition, clofibric acid has also application as an herbicide for plant growth control [3]. Due to its complex structure, conventional biological wastewater treatments are ineffective for its removal [4], thus ending up in several aquatic environments as reported by diverse authors [5-8], where it has an estimated persistence of 21 years [3]. Therefore, alternatives to conventional treatments are required to tackle clofibric acid.

In this context, electro-Fenton stands out as an interesting option. This technique has demonstrated to be effective in the removal of several recalcitrant pollutants that are not efficiently eliminated by biological processes [9], such as various pesticides and pharmaceuticals [10-12]. This is explained in terms of the generation of a powerful oxidation agent, the hydroxyl radical, following the Fenton reaction (Eq. (1)) at an optimal pH of 3. Compared to the Fenton treatment, electro-Fenton has the advantage of *in-situ* generating the hydrogen peroxide (Eq. (2)) and regenerating the ferrous iron at the cathode (Eq. (3)), thus ensuring the availability of the reagents and the continuity of the reaction [13].

$$H_2O_2 + Fe^{2+} \rightarrow {}^{\cdot}OH + OH^- + Fe^{3+} \quad (1)$$

$$O_2 + 2H^+ + 2e^- \rightarrow H_2O_2 \quad (2)$$

$$Fe^{3+} + e^- \rightarrow Fe^{2+} \quad (3)$$

However, achieving a fast and efficient electrogeneration of hydrogen peroxide from the reduction of oxygen is still a challenge for the implementation of electro-Fenton at industrial level [14]. The main limiting factors are the low solubility of oxygen in water under room conditions (approximately 8 mg L^{-1}) and its slow transfer to the cathode [15].

A widespread method to partially overcome those issues is the use of gas diffusion electrodes, where oxygen is supplied directly to the triple-phase interface formed by electrolyte, electrode and gas inlet, thus minimizing mass transfer limitations [16]. However, it suffers from poor oxygen utilization and requires the use of an external compressor [15].

A different approach to increase the saturation level of oxygen is to pressurize the system. According to Henry's law, oxygen solubility in water increases linearly with pressure at low pressures [17]. As a consequence, a hydrogen peroxide production rate as high as 1.84 mmol cm^{-2} h^{-1} was obtained at 30 bar in an undivided cell fed with air [18]. However, it should be noted that the energetic costs associated with the compression needed for pressurizing the system increase with pressure. Moreover, operating at high pressure values requires the use of specific and expensive equipment [15].

An attractive alternative is the use of a jet aerator. This simple and inexpensive device profits from the Venturi effect to supply oxygen to the solution, eliminating the need of a compressor. The air bubbles generated when air is aspired super-saturate in oxygen the electrolyte, thus increasing its transfer to the cathode. This aeration technique has proven to increase the limiting current density to produce hydrogen peroxide [19]. Additionally, the combination of the jet with moderate pressures prompted the pressurized jet aerator, which demonstrated to have a synergistic effect in oxygenating the solution [15,20]. Despite the promising results provided by this powerful aeration system for the electrogeneration of hydrogen peroxide, it has not yet been tested for electro-Fenton.

In a previous work, we have reported the degradation of clofibric acid by a heterogeneous electro-Fenton treatment at bench scale, using the jet aerator coupled with a microfluidic flow-through cell and a fluidized-bed reactor [21]. The aim of the present work is to go one step further, by exploring the effect of combining the mentioned reaction system with pressure, only scarcely reported at lab-scale reactors [22,23]. The combination of pressure and heterogeneous

catalysis for electro-Fenton at bench scale has not been studied in depth previously and consequently, modelling the system behavior was found of utmost interest. To this end, experimental data were used to develop a mathematical model of the bench-scale system, a useful tool for the future simulation of different operational conditions.

2. MATERIALS AND METHODS

2.1. Reagents

2-(p-Chlorophenoxy)-2-methylpropionic acid (clofibric acid, 97%), sodium sulfate, titanium(IV) oxysulfate solution (1.9-2.1%), polytetrafluoroethylene (a 60% wt. Teflon® emulsion solution in H_2O), iron(III) sulfate hydrate, methanol, formic acid and sulfuric acid were supplied by Sigma-Aldrich. Carbon black (Vulcan® XC72) was purchased to Cabot Corporation, sodium alginate was provided by Analema and isopropanol was supplied by VWR Chemicals. All aqueous solutions were prepared with Milli-Q water.

2.2. Experimental setup

Experiments were carried out in a bench-scale closed-circuit system operated at atmospheric pressure and at pressurized conditions of 1 bar and 2 bar of gauge pressure. The setup consisted on several elements: 1) a biphasic tank, which was partially filled with the solution, containing air in its upper part; 2) a pump, that provided a constant flow rate of 140 L h^{-1}; 3) a jet aerator, where the pressure drop caused the aspiration of gas from the top of the tank; 4) a microfluidic flow-through electrochemical cell, with an anode-cathode layout; 5) a fluidized-bed reactor that contained the catalyst for the heterogeneous electro-Fenton assays; 6) a heat exchanger to maintain the solution temperature at 22 ºC, and 7) a compressed oxygen cylinder to pressurize the system. A schematic representation of the installation is shown in the graphical abstract, and more detailed information can be found elsewhere [21].

In the electrochemical cell, the electrodes were separated by a 150 μm PTFE insulating layer. The anode was a boron-doped diamond electrode coated on a niobium mesh (Diachem®,

supplied by Condias GmbH). The cathode was elaborated by depositing onto each side of a titanium mesh (Xian Howah Technology Co., Ltd.) a 100 mL mixture of 1 g L^{-1} of carbon black and 5 g L^{-1} of polytetrafluoroethylene dispersed into isopropanol. The procedure was described in detail elsewhere [21]. Both electrodes were 8 x 9.5 cm, with a wet geometrical area of 33 cm^2 and a surface area of 49.5 cm^2 determined in a previous study [24].

For hydrogen peroxide generation assays, the installation was filled with 2.7 L of a 0.05 M Na_2SO_4 solution. For the electro-Fenton experiments, in addition to the electrolyte, the solution contained 10 mg L^{-1} of clofibric acid, pH was adjusted to 3.0 with sulfuric acid and 6 g of the catalyst were introduced in the fluidized-bed reactor. The iron containing-alginate beads were fabricated based on a previous method [25]. In short, a solution containing 2% w/v of sodium alginate was dropped into an agitated 0.05 M Fe^{3+} solution to produce the cross-linking. The formed spheres were kept 1 h in that hardening solution and then were washed with distilled water and stored at 4ºC in water.

2.3. Analytical methods

Hydrogen peroxide production was followed with a colorimetric technique consisting on forming a complex between H_2O_2 and Ti^{4+}, using a titanium (IV) oxysulfate solution [26]. The absorbance of the complex was measured in a Shimadzu UV-1700 Spectrophotometer at a wavelength of 410 nm.

Clofibric acid was quantified by high performance liquid chromatography (HPLC) with an Agilent 1200 series equipment and a DAD detector connected to a ZORBAX Eclipse Plus C18 column kept at 25ºC. Measurements were done at 225 nm. The mobile phase, 60:40 MeOH:H_2O with 0.1% of formic acid, was pumped at a flow rate of 1 mL min^{-1}.

Carboxylic acids were measured by HPLC using an Agilent 1100 equipment and a DAD detector connected to the output of an ion-exclusion column (Rezex^{TM} ROA-Organic Acid H+ (8%)) kept at 60ºC. The detection was performed at a wavelength of 206 nm. The mobile phase consisted on a 2.5 mM H_2SO_4 solution that flowed at 0.5 L min^{-1}.

Dissolved iron was determined by means of a Varian Liberty RL sequential inductively coupled plasma atomic emission spectroscopy (ICP-AES), using Ar at approximately 10000 K. Samples were diluted 50:50 v/v using NH_4NO_3 to ensure the total solubility of iron. The same procedure was followed to determine the iron content of the alginate beads, after performing an acid digestion of the catalyst.

2.4. Specific energy consumption

The energy consumption was calculated referred to the amount clofibric acid (EC_{CA}) in Eq. (4) and to the amount of hydrogen peroxide ($EC_{H_2O_2}$) in Eq. (5), where E_{cell} is the average cell voltage (V), I the current intensity (A), t the electrolysis time (h), V the solution volume (L), ΔC_{CA} the difference in clofibric acid concentration at time t respect to the initial concentration (mg L^{-1}) and $C_{H_2O_2}$ the concentration of hydrogen peroxide at time t (mg L^{-1}).

$$EC_{CA} = \frac{E_{cell} \cdot I \cdot t}{V \cdot \Delta C_{CA}} \quad (4)$$

$$EC_{H_2O_2} = \frac{E_{cell} \cdot I \cdot t}{V \cdot C_{H_2O_2}} \quad (5)$$

3. RESULTS AND DISCUSSION

3.1. Experimental

3.1.1. *Hydrogen peroxide generation*

As mentioned in the introduction, the *in-situ* formation of hydrogen peroxide is key for the electro-Fenton treatment. Hence, before testing the degradation of clofibric acid, the capability of the installation with the pressurized jet aerator to electrogenerate hydrogen peroxide was analyzed.

Low relative pressures, namely 0, 1 and 2 bar, were selected in order to reduce the costs and avoid the use of more expensive high-pressure specific equipment, because the goal was to check the potential advantages of working at pressures over atmospheric pressure. Results

showed that hydrogen peroxide production is significantly boosted by the application of pressure to the system (Fig. 1a). At atmospheric pressure (gauge pressure of 0 bar), the accumulation of the product reached a plateau after approximately 3 h of experiment, being the maximum accumulation of 22 mg L^{-1}. However, for gauge pressures of 1 and 2 bar, the maximum amounts obtained were considerably higher: 136 and 197 mg L^{-1}, respectively. Interestingly, for those pressures, the concentration had not yet achieved the equilibrium even after 5 h, indicating that the system would have the capacity to further generate and accumulate hydrogen peroxide. The reason behind this considerable enhancement of hydrogen peroxide production is two-fold: the linear increase in oxygen solubility with pressure, according to Henry's law [27], and the higher mass flow of oxygen entering the jet, thanks to the higher density of the gas under pressure [15].

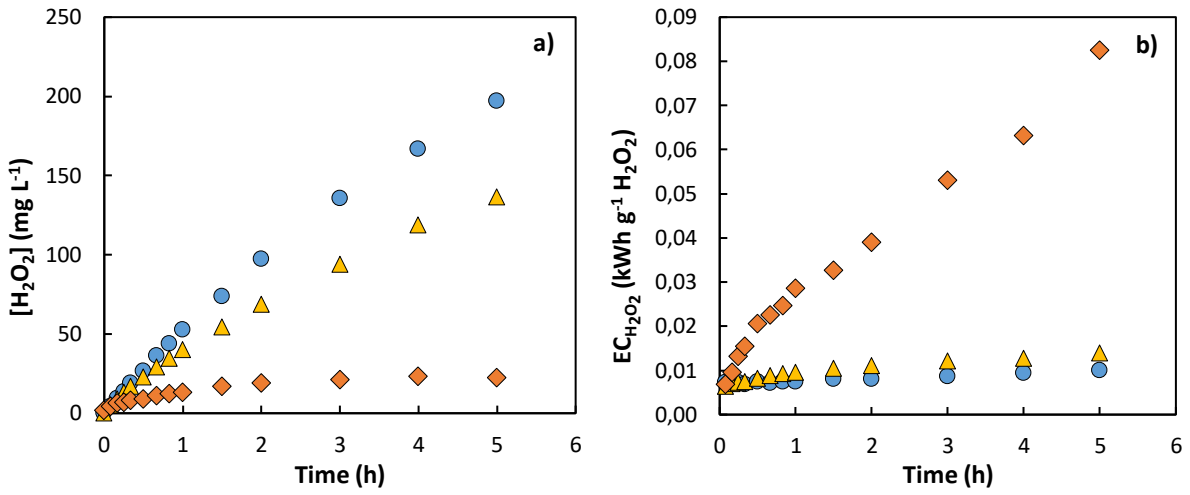

Fig. 1. Hydrogen peroxide generation (a) and specific energy consumption (b) at 0.25 A under 0 (◆), 1 (▲) and 2 (●) bar of gauge pressure.

Although the hydrogen peroxide concentrations obtained with the pressurized installation are considerably high, it is possible to find in literature higher values in systems operated at atmospheric pressure. However, in order to determine which system is better from an actual implementation point of view, the hydrogen peroxide electrogeneration data should be analyzed in detail. Some examples of high hydrogen peroxide productions obtained with carbon-based

cathodes reported in literature are summarized in Table 1. As it can be observed, hydrogen peroxide concentrations range from 102 g L^{-1} to 22 mg L^{-1}, but the working volume and other parameters considerably differ; hence, hydrogen peroxide production rates are provided for comparison purposes.

Table 1. Comparison of hydrogen peroxide electrogeneration reported in literature.

Cathode material[a]	**Cathode area**	**H_2O_2 (mg L^{-1})**	**Working volume (L)**	**H_2O_2 production rate (mg cm^{-2} h^{-1})[b]**	**Specific consumption (kWh g^{-1} H_2O_2)**	**Operational conditions**	**Ref.**
CB based GDE	Surface: 64 cm^2	102000 (≈3 M)	0.25	30.60	-	Divided cell, 0.2 M H_2SO_4 + 0.5 M K_2SO_4 + 0.01 M TBABr, pH 1.4, 110 mA cm^{-2}, fed with O_2	[28]
CB/PTFE based GDE	Geometric: 20 cm^2	3370	0.4	44.93	0.008	Undivided cell, 1 M KOH, alkaline pH, -1.1 V vs. Ag/AgCl, fed with O_2 0.2 bar	[29]
CB/MWCNT/PTFE based GDE	Surface: 28.3 cm^2	1002.4	0.1235	1.46	-	0.05 Na_2SO_4 , 3.5 mA cm2, fed with O_2	[30]
CB/PTFE/carbon fiber based GDE	Geometric: 2 x 7 cm^2 (ø 3 cm)	566	0.2	2.70	0.0086	Undivided cell, 0.05 M Na_2SO_4, pH 7, 7.1 mA cm^{-2}, air flow 0.5 L min^{-1}	[31]
CNT/PTFE/GF based GDE	Geometric: 4.9 cm^2 (ø 2.5 cm)	486.2 (14.3 mM)	0.25	4.95	-	Undivided cell, 0.05 M Na_2SO_4, pH 3, 100 mA (20 mA cm^{-2}), O_2 flow 140 mL min^{-1}	[32]
AC/PTFE/GF based GDE		200.6 (5.9 mM)		2.04	-		
CB/PTFE/CF	Geometric: 50 cm^2	583	1	5.83	-	Undivided cell, 0.05 M Na_2SO_4, 20 mA cm^{-2}, fed with air	[19]
CB/PTFE/CF	Geometric: 60 cm^2	180	0.15	0.06	-	Undivided cell, 0.05 M Na_2SO_4, pH 3.4, 150 mA (2.5 mA cm^{-2}), fed with air	[33]
RVC 100ppi	Geometric: 5 cm^2 (2x2.5 cm)	≈ 475	0.1	1.90	-	Divided electrochemical cell, Na_2SO_4/$NaHSO_4$ buffer, pH 2.5, 35 mA (7 mA cm^{-2}), O_2 flow 200 mL min^{-1}	[34]
GF	Geometric: 10 cm^2	128.1	0.1	1.28	0.00799	Divided electrochemical cell, 0.05 M Na_2SO_4, pH 4.2, 4 mA cm^{-2}, air flow 40 mL min^{-1}	[35]
Aluminium foam/CB/PTFE	Geometric: 33 cm^2 (16.5 cm^3)	≈22	2.25	3.15 (6.3 mg h^{-1} cm^{-3} x 0.5 cm)	0.0036	Pressurized undivided cell, 0.05 M Na_2SO_4, 10 mA cm^{-3} (5 mA cm^{-2}), 6 bar	[20]

CB/PTFE/Ti mesh	Surface: 49.5 cm^2	197	2.7	2.15	0.00920	Pressurized undivided cell, 0.05 M Na_2SO_4, natural pH, 250 mA (5 mA cm^{-2}), fed with O_2, 2 bar	This study

[a] AC: Activated carbon; CB: Carbon black; CF: Carbon felt; CNT: Carbon nanotubes; GDE: Gas diffusion electrode; GF: Graphite felt; MWCNT: Multi-walled carbon nanotubes; PTFE: polytetrafluoroethylene: RVC: Reticulated vitreous carbon. [b] Calculated with the available data when not provided in the article.

An impressive amount of 102 g L^{-1} (corresponding to 30.6 mg cm^{-2} h^{-1}) was achieved by Kolyagin and Kornienko using a gas diffusion electrode (GDE) [28]. It should be noted though that this value was attained in a divided electrochemical cell, which achieves higher hydrogen peroxide concentrations thanks to avoiding its anodic oxidation. However, this configuration presents several drawbacks, such as higher operation costs because of the increased cell potential and more complicated handling: additionally, this setup is not recommended for water remediation, due to the inefficient use the potential of the electrochemical system given that the reactivity of the anode towards the pollutant abatement is neglected [36]. In general, the higher hydrogen peroxide concentrations presented in Table 1 correspond to GDE, which have been confirmed as highly efficient electrodes towards the electrogeneration of this reagent. And yet, some of the production rates are similar or even lower than the one reported in our investigation [30-32]. In any case, it should be taken into consideration that GDE enhance the complexity and cost of the cell, and make it more difficult to develop the process on an applicative scale [17,37]. By contrast, the setup presented in this investigation already operates at bench scale and it is easily scalable. Additionally, it is operated under moderate pressures, and so it seems suitable from an industrial point of view, since gauge pressures up to 10 bar are easily managed with conventional commercial electrochemical cells and require very low energetic costs for compression [17]. Furthermore, the hydrogen peroxide production rate obtained in the present study is in the range of those reported with typical carbon-based cathode materials when no GDE are used (0.06-5.83 mg cm^{-2} h^{-1}) [19,20,33-35]. Considering all this, the installation proposed in this research can efficiently achieve hydrogen peroxide production rates that are

competitive compared with other systems reported in the literature while at the same time the setup configuration has potential for a future industrial implementation.

Regarding the specific energy consumption, a drastic reduction with pressure was observed (Fig. 1b). The results obtained are slightly higher but close enough to the minimum reported by a previous research on the pressurized jet aerator, which obtained the lowest energy consumption up to that point in acid medium [20]. In that study, at 10 mA cm^{-3} (equivalent to 5 mA cm^{-2}, calculated with the 5 mm thickness of the electrode) and a gauge pressure of 6 bar, the electric consumption was 0.0036 kWh g^{-1} H_2O_2, whereas in the present work, with 0.25 A (equivalent to 5 mA cm^{-2}, obtained with the electrode surface area) and 3 times lower pressure, the energy consumption was 0.0092 kWh g^{-1} H_2O_2, which also becomes a very interesting value as compared to the range of consumptions reported in that investigation (0.0036 - 0.0254 kWh g^{-1} H_2O_2) and in Table 1.

3.1.2. *Electro-Fenton treatment*

Given that pressure increases hydrogen peroxide generation, an improvement in the efficiency of the electro-Fenton treatment may be expected. Therefore, the effect of pressure was tested for the first time for a heterogeneous electro-Fenton process in a bench-scale setup, as far as the authors are aware. The installation used in our previous study ([21]) was pressurized this time, analyzing the improvements achieved in clofibric acid degradation with the combined pressurized jet aerator system.

Two different current intensities were selected, 0.12 A and 0.25 A. The obtained results are depicted in Fig. 2a and Fig. 2b, respectively, and the pseudo-first order kinetic constants are presented in Table 2. The process was always faster at 0.25 A than at 0.12 A, regardless of the pressure applied. At atmospheric pressure, clofibric acid abatement was almost complete after 8 h, achieving a 97% elimination at the lower current intensity and a 98% at the higher. Regardless of the current intensity, increasing the relative pressure accelerated the degradation

of the pollutant: the abatements obtained at 0 bar were surpassed in just 1 h at 0.25 A and in 3 h at 0.12 A operating at 1 or 2 bar. The enhancements obtained with pressure were more remarkable at 0.25 A: while the degradation rate was roughly doubled when increasing pressure from 0 to 1 bar at 0.12 A, it was increased 5 times when done at 0.25 A.

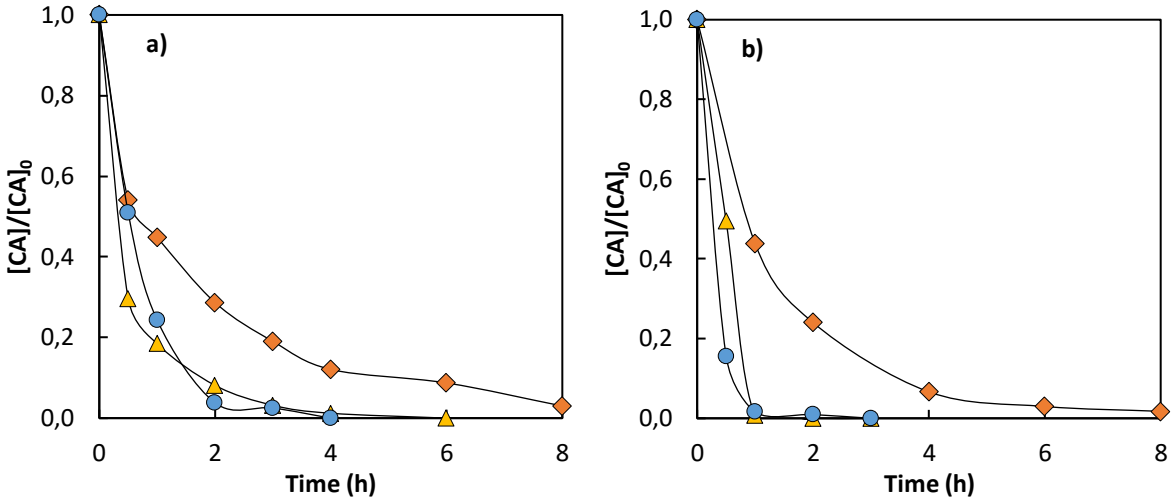

Fig. 2. Clofibric acid (CA) decay during electro-Fenton treatment under different pressures at 0.12 A (a) and 0.25 A (b). 0 (◆), 1 (▲) and 2 (●) bar of gauge pressure

Table 2. Pseudo-first order parameters for the elimination of clofibric acid.

Gauge pressure	0.12 A		0.25 A	
	k (min^{-1})	R^2	k (min^{-1})	R^2
0 bar	0.009	0.929	0.014	0.974
1 bar	0.020	0.939	0.071	0.825
2 bar	0.026	0.991	0.067	0.996

However, surprisingly, even if the increase in relative pressure from 1 to 2 bar provided a higher amount of hydrogen peroxide in the electrogeneration assays, those increases did not reflect such an improvement in the pollutant removal, regardless of the current intensity applied. This seems to imply that the process reaches the maximum rate at 1 bar, and it cannot be considerably improved by rising the pressure. It is important to note that the same catalyst dosage was provided in the different assays, in order to maintain an adequate and comparable fluidity of the alginate beads at the fluidized-bed reactor in all the experiments. As a consequence,

although the molar amount of hydrogen peroxide was higher than that of iron in all assays, given the higher amount of hydrogen peroxide obtained with pressure, the molar ratio between hydrogen peroxide and iron varied, increasing with pressure. Therefore, the fact that clofibric acid removal was not further improved at 2 bar compared to 1 bar might be related to a better ratio between the Fenton reactants at the lower pressure. In this sense, even if a higher concentration of hydrogen peroxide is produced at 2 bar, the catalytic ability of iron towards hydrogen peroxide could be limited by the fixed catalyst dosage at that pressure, becoming the excessive hydrogen peroxide a scavenger of hydroxyl radicals according to Eq. (6) [38]. Additionally, it was also suspected that it might be related to a different behavior of the catalyst with pressure. Because of that, iron leaching was analyzed and will be further discussed in section 3.1.3.

$$H_2O_2 + {}^{\cdot}OH \rightarrow H_2O + HO_2^{\cdot} \quad (6)$$

The degradation of clofibric acid was also evaluated in terms of the specific charge required and specific energy consumption. Values of the clofibric acid removal at a given specific charge of 0.09 A h L^{-1} are presented in Fig. 3a. As it can be observed, increasing the pressure increases the efficient usage of the charge, having a noticeable impact when working at 1 bar respect from atmospheric pressure, but not so remarkable when increasing it from 1 to 2 bar. Regarding the current intensity, the lower value yields better results at atmospheric pressure, obtaining a removal of 71%, while at the higher value of current intensity it is of only of 56%. However, this tendency changes when working above the atmospheric pressure, obtaining the experiments at higher current intensity a higher removal of the pollutant than those at lower ones, for the given specific charge of 0.09 A h L^{-1}. Therefore, this seems to indicate that working with the pressurized system allows to work at higher current intensities without reducing the efficiency of the specific charge usage.

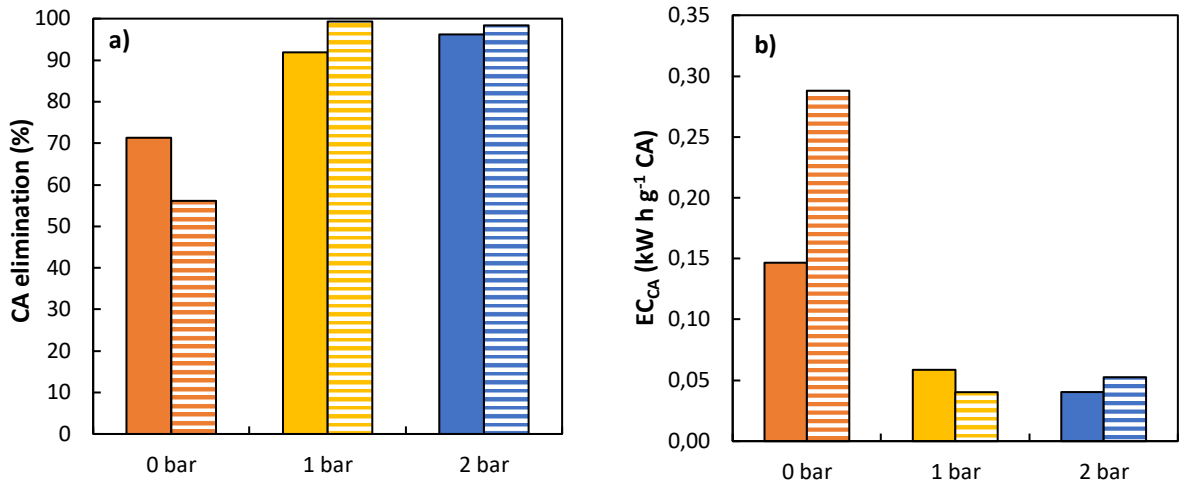

Fig. 3. Clofibric acid (CA) elimination at a specific charge of 0.09A h L^{-1} (a) and specific energy consumption for an elimination of 97-99% (b). ■ 0.12A, ▤ 0.25 A.

Furthermore, the specific energy consumption at the electrochemical cell (not considering the energy consumed by the pump or the compression) for the elimination of clofibric acid was calculated. Results for a removal between 97 and 99% are depicted in Fig. 3b. Energy consumption was remarkably higher at 0 bar, being almost doubled when increasing current intensity from 0.12 A to 0.25 A. Interestingly, working with the pressurized system considerably reduced the specific energy consumption, not showing significant changes between 1 and 2 bar or between the two current intensities analyzed.

Finally, the generation of intermediates at different pressures was analyzed. Some of them, the carboxylic acids (oxalic, succinic and formic acids), were specifically measured, whereas others correspond to peaks detected while measuring clofibric acid by HPLC but were not identified, and thus were not quantified. As shown in Fig. 4, the quantity of compounds measured at atmospheric condition is higher than what was obtained by applying 1 or 2 bar of gauge pressure. In fact, by the end of the treatment all the unidentified intermediates had not yet been completely abated at 0 bar, while in the assays at 1 and 2 bar they were eliminated long before. Regarding the carboxylic acids (the value of the concentration detected is shown in Fig. 4), they still remained after 8 h of treatment even in the pressurized assays. This can be explained by

considering that they are rather resistant to degradation by means of electro-Fenton, and therefore tend to accumulate in the solution as by-products [39].

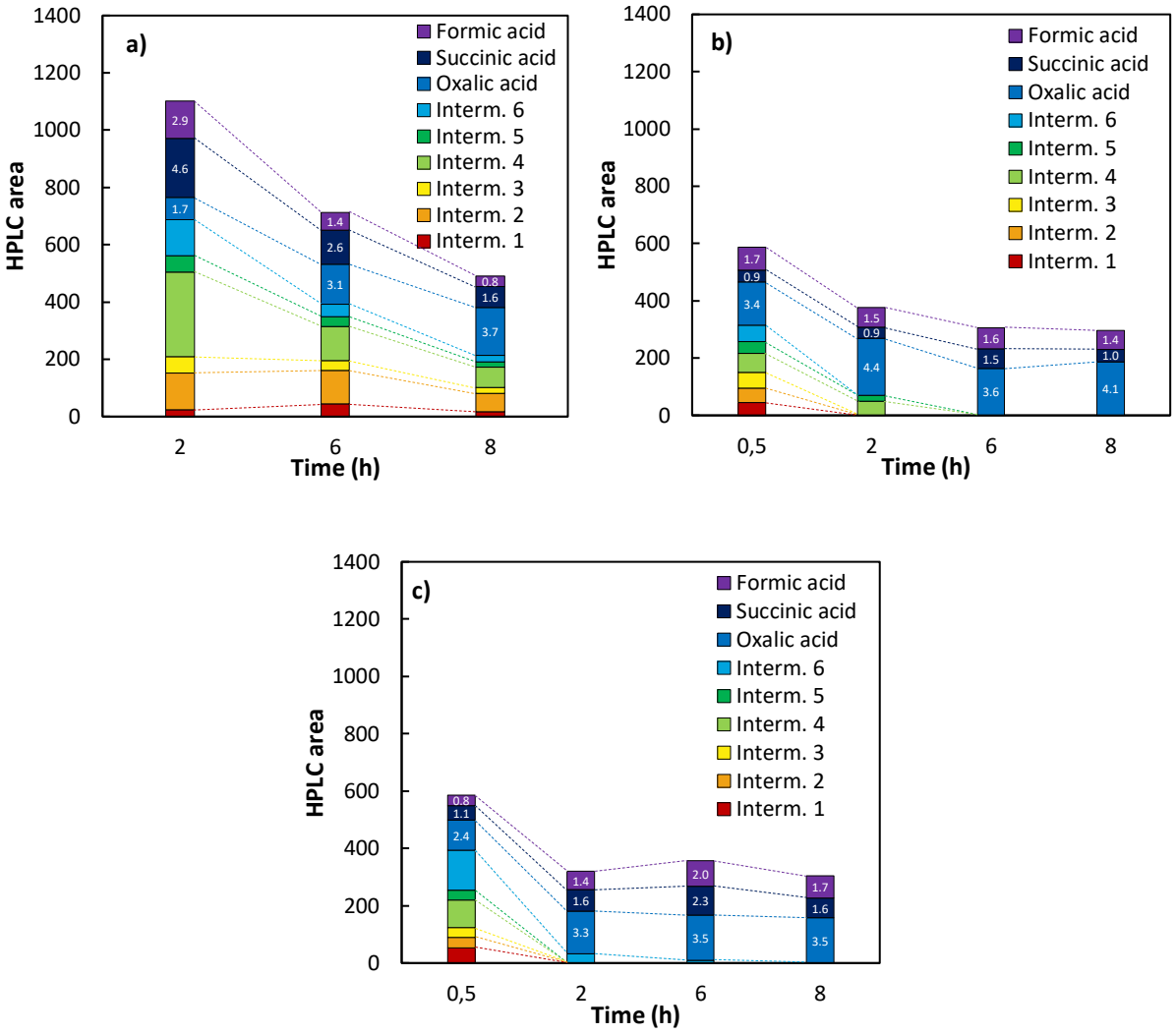

Fig. 4. Intermediates detected by HPLC during the electro-Fenton treatments at 0.25 A and 0 bar (a), 1 bar (b) and 2 bar (c). Intermediates 1-6 are presented in terms of HPLC area, whereas for oxalic, succinic and formic acids their concentration in mg L^{-1} is indicated on the bars.

3.1.3. *Effect of pressure on the catalyst*

Given the nature of the iron alginate beads, a biopolymer matrix where iron is cross-linked, it was found interesting to gain insight into the catalyst behavior with pressure. Therefore, iron

leaching was analyzed. An acid digestion was performed to the catalyst after each assay and the amount of iron detected was compared to that of the raw catalyst. Additionally, the iron dissolved in the solution by the end of the treatment was measured. The outcome of the iron mass balances is depicted in Fig. 5, specifying the proportion of iron detected in the catalyst, detected in the solution and not detected in the catalyst or the solution at the end of each assay.

Results demonstrated that at 0.25 A, regardless of the pressure, around a 70% of the initial iron content still remained in the catalyst after 8 h of electro-Fenton treatment (Fig. 5a, b and c). Therefore, it can be concluded that working at moderate pressures does not damage the alginate-beads nor increases the iron leaching, compared with working at atmospheric condition.

It should be mentioned, though, that even if the amounts of iron leached were practically the same at the evaluated pressures, the distribution of that iron seems to be different with pressure. Dissolved iron decreases as pressure increases, while the amount of unmeasured iron rises (Fig. 5a, b and c). That unmeasured iron is believed to be precipitated at the cathode, where solid traces were detected.

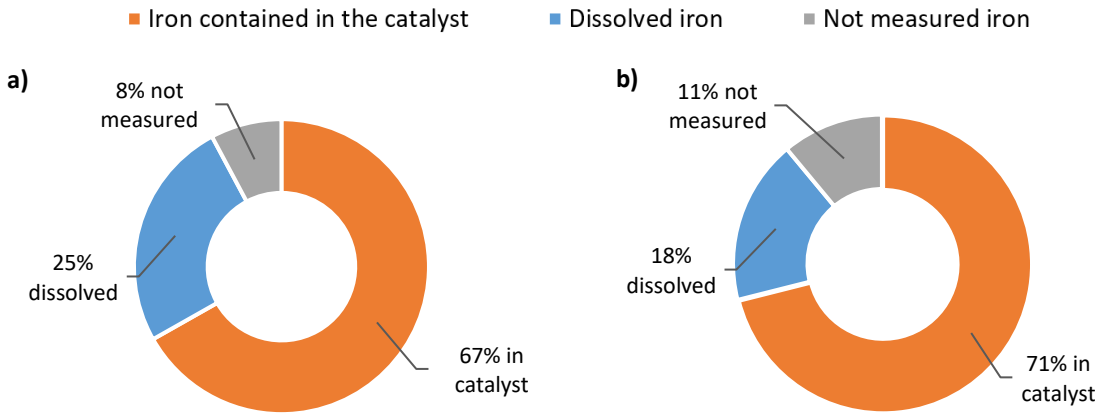

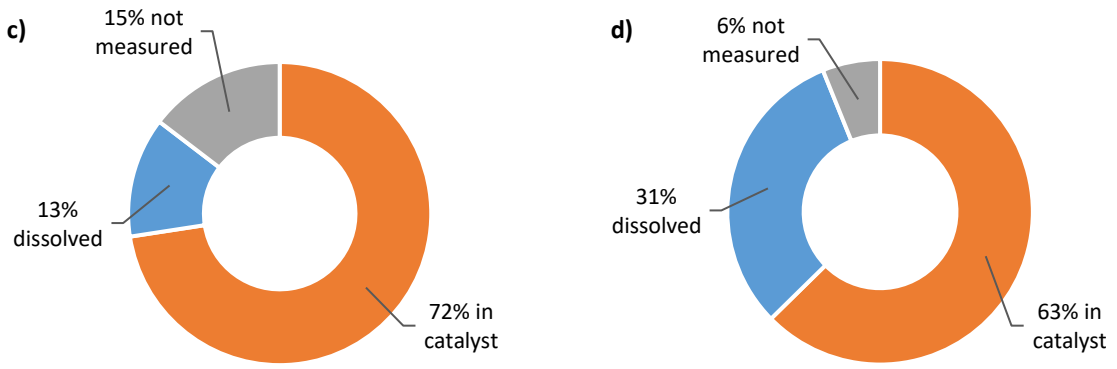

Fig. 5. Distribution of iron after the electro-Fenton assays at 0.25 A and 0 bar (a), 1 bar (b), 2 bar (c) and 0.12 A and 1 bar (d).

Interestingly, the color of the precipitate changed from orange at 0 bar, suggesting the formation of ferric compounds, to greenish at 2 bar, associated with the formation of ferrous compounds. These findings are contrary to what was expected since the greater amount of oxygen allegedly present at higher pressures should transform the ferrous ion into the ferric ion. However, that behavior is in line with what observed in the degradation of clofibric acid, where the elimination was not improved at 2 bar as compared to 1 bar. Apparently, an excess in hydrogen peroxide at 2 bar might be favoring the transformation of Fe(III) to Fe(II) at the cathode precipitate according to Eq. (7), which is part of the Fenton cycle [39]. On the other hand, the greater amount of precipitate obtained at higher pressures might be reducing the active sites available for hydrogen peroxide electrogeneration thus preventing the formation of a higher amount of hydroxyl radicals to attack the pollutant. Whatever the case, the precipitate deposited at the cathode might be reducing the hydrogen peroxide available, but it is not clear if that is the cause of the unimproved clofibric acid abatement at 2 bar compared with 1 bar, or if it does not have an impact on the pollutant removal because there is an excess of hydrogen peroxide at 2 bar. A deeper investigation should be performed to clarify this behavior, but it seems clear that the operation at 1 bar is more efficient.

$$Fe^{3+} + H_2O_2 \rightarrow Fe^{2+} + HO_2^{\cdot} + H^+ \quad (7)$$

Finally, regarding the current intensity, at 0.12 A and 1 bar (Fig. 5d) the ratio of dissolved iron vs. unmeasured iron is more than 3 times higher than at 0.25 A. The reduced amount of undetected iron, presumably precipitated at the cathode, at lower current intensities is explained due to a minor basification of the cathode.

3.2. Mathematical model

Given that, to the best of the authors' knowledge, this is the first time for which the combination of a pressurized jet aerator and a fluidized-bed reactor at bench scale is reported, it was deemed important to mathematically represent the system's behavior to gain a deeper understanding. Obtaining a model of the system could provide a useful tool to simulate different operational conditions and help in scaling-up the treatment in future investigations.

Therefore, a mathematical model is proposed in this Section, using the experimental data of this research to fit the model parameters. This model aims to represent the variation in the concentration with time of the dissolved oxygen, hydrogen peroxide and clofibric acid within the reaction system operated in batch mode. All the variables and parameters used in the model, along with their units, have being collected in Table 3. In the following sections the equations of the model will be presented.

Table 3. Parameters and variables used in the mathematical model.

Term	Meaning	Units
A	Electrode surface area	m^2
C_{Fe}	Concentration of iron	mol L^{-1}
C_{j_i}	Concentration of compound j at time i, being j O_2, H_2O_2, clofibric acid or scavenger species	mol L^{-1}
$C_{O_2 sat}$	Concentration of O_2 at saturation	mol L^{-1}
C_{lim}	Limiting clofibric acid concentration	mol L^{-1}

Term	Meaning	Units
F	Faraday constant	C mol^{-1} e^-
I	Current intensity	A
k	Constant in H_2O_2 generation performance parameter	mol O_2 L^{-1}
k_{CA}	Pseudo-first order kinetic constant for clofibric acid	min^{-1}
k_d	H_2O_2 decomposition kinetic constant	min^{-1}
k_{Fen}	Second order kinetic constant for Fenton reaction	L min^{-1} mol^{-1}
k_m	Mass transfer coefficient for O_2	m s^{-1}
k_{sc}	Second order kinetic constant for scavenger species	
n_{CA}	Number of electrons consumed per molecule of clofibric acid consumed	mol e^- mol^{-1} $^{\cdot}OH$
$n_{H_2O_2}$	Number of electrons consumed per molecule of H_2O_2 electrogenerated	mol e^- mol^{-1} H_2O_2
n_{sc}	Number of electrons consumed per molecule of scavenger generated	mol e^- mol^{-1} scavenger
t	Time	min
V	Volume	L
η_i	H_2O_2 electrogeneration performance at time *i*	

3.2.1. *Modelling hydrogen peroxide generation*

First, hydrogen peroxide production in the system is represented, assuming a constant volume in the reactor. To model its generation and destruction, the mass balance shown in Eq. (8) is proposed. It consists of four terms: the first of them stands for hydrogen peroxide electrochemical generation; the second, third and fourth represent its consumption, corresponding the second to hydrogen peroxide decomposition in parasitic reactions, the third to its consumption when directly oxidizing clofibric acid and the latter to its consumption in the Fenton reaction creating hydroxyl radicals. On the other hand, the variation in the concentration of dissolved oxygen, on which the electrogeneration of hydrogen peroxide relies, was modelled based on the mass balance shown Eq. (9). As it can be observed, it consists of two terms: the first one represents the transport of the oxygen gas into the solution, which is limited by the

saturation concentration of dissolved oxygen, and the second one stands for the disappearance of oxygen during the electrogeneration of hydrogen peroxide (other reactions involving O_2 generation or consumption have been neglected).

$$V \cdot \frac{dC_{H_2O_2}}{dt} = \frac{I}{n_{H_2O_2} \cdot F} \cdot \eta - k_d \cdot C_{H_2O_2} \cdot V - k_{H_2O_2} \cdot C_{H_2O_2} \cdot C_{CA} \cdot V - k_{Fen} \cdot C_{Fe} \cdot C_{H_2O_2} \cdot V \quad (8)$$

$$V \cdot \frac{dC_{O_2}}{dt} = k_m \cdot A \cdot \left(C_{O_2sat} - C_{O_2}\right) - \frac{I}{n_{H_2O_2} \cdot F} \cdot \eta \quad (9)$$

When the Euler finite elements method is applied to Eqs. (8) and (9), Eqs. (10) and (11) are obtained, respectively. It should be mentioned that conversion factors were introduced in those equations to make units consistent when using the units mentioned in Table 3 for each parameter (60 s min^{-1} in Eqs. (10) and (11), and 1000 L m^{-3}·60 s min^{-1} in Eq. (11)). As it can be observed, both equations are related by the H_2O_2 electrogeneration performance, η_t (Eq. (12)), which is roughly proportional to the oxygen concentration for low values of concentration respect to the constant k, but as the concentration increases, it gets closer to 1.

$$C_{H_2O_2\,t+1} = C_{H_2O_2\,t} + \frac{\Delta t}{V} \cdot \left(\frac{I \cdot 60}{n_{H_2O_2} \cdot F} \cdot \eta_t - k_d \cdot C_{H_2O_2\,t} \cdot V - k_{H_2O_2} \cdot C_{H_2O_2\,t} \cdot C_{CA_t} \cdot V - k_{Fen} \cdot C_{Fe} \cdot C_{H_2O_2\,t} \cdot V\right) \quad (10)$$

$$C_{O_2\,t+1} = C_{O_2\,t} + \frac{\Delta t}{V} \cdot \left(k_m \cdot A \cdot 60000 \cdot \left(C_{O_2sat} - C_{O_2\,t}\right) - \frac{I \cdot 60}{n_{H_2O_2} \cdot F} \cdot \eta_t\right) \quad (11)$$

$$\eta_t = \frac{C_{O_2\,t}}{k + C_{O_2\,t}} \quad (12)$$

The proposed equations (Eqs. (10)-(12)) were defined in a spreadsheet and changes in the concentrations of dissolved oxygen and hydrogen peroxide with time during hydrogen peroxide

electrogeneration were modelled for each relative pressure. For doing so, k_d (from Eq. (10)) and k (from Eq. (12)) were used as fitting parameters, adjusting the model to the experimental data using the least squares method, setting as the objective to minimize the square errors between the estimated hydrogen peroxide concentrations and the experimental data. Given that in hydrogen peroxide electrogeneration assays no iron or clofibric acid are added (C_{CA_t} = 0, C_{Fe} = 0), the terms representing H_2O_2 disappearance due to its reaction with clofibric acid or due to the Fenton reaction in Eq. (9) do not play any role in the parameter estimations carried out in this section. It should be mentioned that the mass transfer coefficient, k_m, was obtained experimentally following the limiting-current technique as described elsewhere [40].

The results obtained with the modelling are represented in Fig. 6, and the values of the fitting parameters in Table 4. Fig. 6a presents the modelled dissolved oxygen concentration. It should be noted that since no dissolved oxygen measurements were performed during the assays, the modelled concentrations could not be compared with empirical data, but just validated in terms of the hydrogen peroxide generation data. As observed therein, the concentration depends on pressure since the saturation value increases when rising the pressure. It is worth mentioning that the installation is pressurized with compressed oxygen gas, and so the maximum solubility of oxygen when working under pressure differs from that of a system pressurized with air, given that the equilibrium concentration of dissolved oxygen is proportional to the oxygen partial pressure in the supply gas [41]. This fact has been taken into consideration when calculating the saturation concentrations, which are represented in Fig. 6a as horizontal dotted black lines.

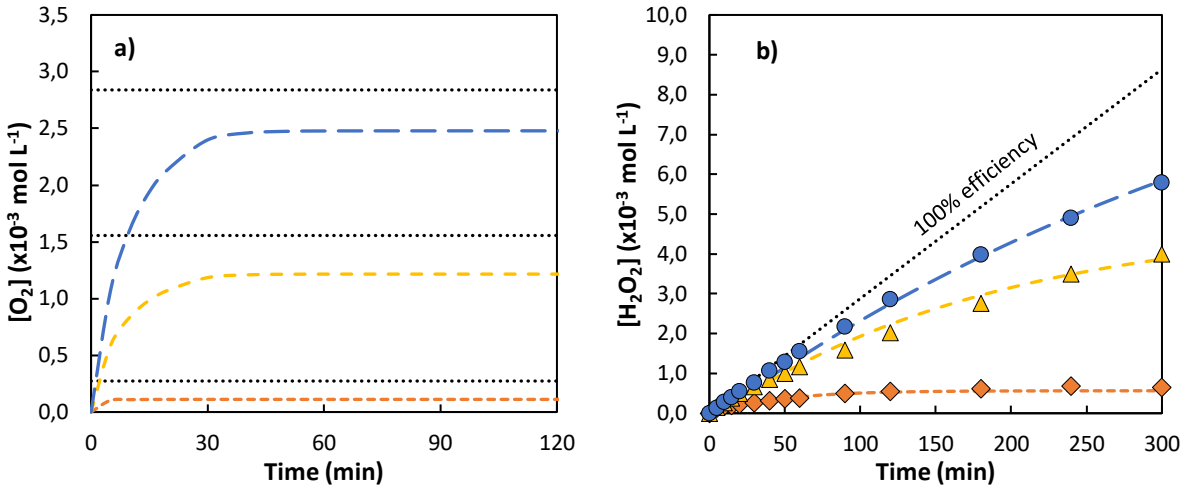

Fig. 6. Estimation of dissolved oxygen concentration (a) and estimation of hydrogen peroxide concentration vs. experimental data (b) in hydrogen peroxide generation assays. Input data for the model: Δt = 10 min; V = 2.7 L; I = 0.25 A; $n_{H_2O_2}$ = 2; F = 96485 C mol^{-1} e$^-$; C_{CA_t} = 0 mol L^{-1}; k_m = 6.84·10^{-4} m s^{-1}; A = 4.95·10^{-3} m^2; C_{O_2sat} = 2.73·10^{-4}, 1.56·10^{-3} and 2.84·10^{-3} mol L^{-1} for 0, 1 and 2 bar (dotted line in a). Symbols are experimental data and dashed lines are estimations at 0 (◆, ----), 1 (▲, - - -) and 2 (●, — —) bar of gauge pressure.

Table 4. Parameters obtained after fitting the model.

Fitting parameter	Value obtained at		
	0 bar	1 bar	2 bar
k_d (min^{-1})	0.0215	0.0053	0.0023
k $(mol\ O_2\ L^{-1})$	1.52·10^{-4}		

Additionally, the fitting of the estimated hydrogen peroxide concentration in the system with the experimental data obtained in electrogeneration assays performed at 0.25 A is shown in Fig. 6b. The fitting was obtained for a k, the constant in Eq. (12), of 1.52·10^{-4} mol O_2 L^{-1}. Since this parameter does not depend on pressure, a unique value was set for all the pressures. On the contrary, if only one decomposition kinetic constant, k_d, was used, the modelled hydrogen peroxide generation did not faithfully represent the data observed in the laboratory experiences.

Thus, a value for each pressure was obtained, which suggests that an increase in pressure leads to a slower decomposition rate (Table 4). There could be two reasons for understanding this inverse relationship between pressure and hydrogen peroxide decomposition rate. On the one hand, current efficiency for the electrogeneration of hydrogen peroxide rises with pressure (curves get closer to the 100% efficiency in Fig. 6b). Given that the same current intensity is used for all the different pressure scenarios, at higher pressures the available electrons for other reactions, such as the consumption of hydrogen peroxide by cathodic reduction (Eq. (13)), are lower. Therefore, hydrogen peroxide decomposition by this means becomes less important as pressure increases. In a similar way, Scialdone et al. [18] noticed that the generation of H_2 by the cathodic reduction of water, another parasitic reaction requiring electrons, was decreased as pressure (and consequently H_2O_2 generation) was enhanced. On the other hand, the fact that the solution is super-saturated with oxygen might also explain why the decomposition diminishes with pressure. Taking into consideration that hydrogen peroxide can also be consumed by disproportionation (Eq. (14)) and anodic oxidation (Eq. (15)), the remarkable increase in the oxygen available in the solution with pressure might not promote the abovementioned reactions. Instead, since those degradation reactions have oxygen as a product, the equilibrium might be shifted to the H_2O_2 side, according to the Le Chatelier's principle.

$$H_2O_2 + 2e^- + 2H^+ \rightarrow 2H_2O \quad (13)$$

$$2H_2O_2 \rightarrow O_2 + 2H_2O \quad (14)$$

$$H_2O_2 \rightarrow O_2 + 2H^+ + 2e^- \quad (15)$$

3.2.2. *Modelling electro-Fenton treatment*

Once hydrogen peroxide estimations proved to faithfully represent the actual amount generated during the electrogeneration assays, the next step was to model the electro-Fenton treatment. In order to assess the role of hydrogen peroxide during the electro-Fenton treatment of clofibric acid, some basic experiments were performed. Firstly, assays where hydrogen peroxide and

clofibric acid were mixed at different ratios were analyzed, in the absence of iron and electric field. However, clofibric acid concentration was not reduced during those experiments, suggesting that hydrogen peroxide is not capable of directly oxidizing clofibric acid (results not shown). Hence, this indicates that $k_{H_2O_2} \approx 0$ (the third term in Eq. (10) does not actually play a role in hydrogen peroxide abatement), and so hydrogen peroxide disappearance due to its direct reaction with clofibric acid is not likely to occur during electro-Fenton assays. Then, Fenton assays were performed, in the absence of electric field. In this case, a degradation of the pollutant was observed (data not shown), which is explained by the presence of iron in the solution that reacted with hydrogen peroxide yielding the generation of hydroxyl radicals. The different ability of hydrogen peroxide and the hydroxyl radicals to degrade the pollutant can be explained in terms of their oxidation potential. Hydroxyl radicals have a strong oxidation capacity (E° = 2.80 V vs. SNE), with a higher oxidation potential compared to hydrogen peroxide (E° = 1.77 V vs. SNE) or other reactive oxygen species (such as ozone E° = 2.07 V vs. SNE or molecular oxygen E° = 1.23 V vs. SNE) [42].

Considering this, a similar behavior was expected during the electro-Fenton treatment where, even if other oxidizing species were generated, it was assumed that hydroxyl radicals were the main responsible for the degradation of clofibric acid, which is in line with what reported by several authors in the electro-Fenton treatment of other organic pollutants [43-46]. Bearing this in mind, the concentration of clofibric acid within the reactor is represented by its mass balance shown Eq. (16), where the first term represents the chemical elimination of the pollutant due to the presence of hydroxyl radicals that attack clofibric acid, and the second term stands for its electrochemical degradation by means of anodic oxidation (enhanced with the use of a very efficient boron-doped diamond anode). It should be noted that the kinetics of the reaction between clofibric acid and hydroxyl radicals was considered to be of pseudo first order, given that hydroxyl radicals are very reactive species whose concentration reaches a steady-state during electrolysis and do not accumulate [47]. Hence, k_{CA} represents the apparent rate

constant, which is equal to $k_{CA_{abs}} \cdot C_{\cdot OH}$, being $k_{CA_{abs}}$the absolute rate constant and $C_{\cdot OH}$ the concentration of hydroxyl radicals. After applying to Eq. (16) the Euler finite elements method, Eq. (17) is obtained. Using the values of parameters k and k_d obtained in the previous section (Table 4), assuming a $n_{CA} = 1$ and taking the Fenton rate constant value from literature ($k_{Fen} = 63\ M^{-1}\ s^{-1}$ [39]), the behavior of the electro-Fenton treatment was modelled with Eqs. (10), (11), (12) and (17) by applying the method of least squares, minimizing the square residuals of clofibric acid and hydrogen peroxide experimental concentrations compared with the modelled ones.

$$V \cdot \frac{dC_{CA}}{dt} = -k_{CA} \cdot C_{CA} \cdot V - \frac{I}{n_{CA} \cdot F} \cdot \frac{C_{CA_t}}{C_{lim}} \quad (16)$$

$$C_{CA_{t+1}} = C_{CA_t} + \frac{\Delta t}{V} \cdot \left(-k_{CA} \cdot C_{CA_t} \cdot V - \frac{I \cdot 60}{n_{CA} \cdot F} \cdot \frac{C_{CA_t}}{C_{lim}} \right) \quad (17)$$

Although clofibric acid decay was accurately fitted by the model proposed so far, it was noticed that the trend observed in hydrogen peroxide during the electro-Fenton treatment was not correctly modelled. In assays at 1 and 2 bar, hydrogen peroxide did not follow the typical tendency where it initially accumulates to eventually reach a stabilization state caused by the balance between its generation and its destruction. Instead, at those gauge pressures, a decay in hydrogen peroxide was observed after 2 h (Fig. 7a, symbols). This behavior can only be explained by the presence of scavenger species that are consuming hydrogen peroxide. Apart from iron, that consumes it in the Fenton reaction (Eq. (1)), there can be other scavengers attacking hydrogen peroxide, such as radicals or other oxidants like ozone (which can be formed from oxygen oxidation at acidic conditions [48]). It is well known that ozone reacts with hydrogen peroxide to form radicals, which enhance the degradation of organic compounds. But when those radicals do not have enough organic matter to oxidize, they recombine or propagate in chain reactions, thus consuming the present oxidants. This explains the observed hydrogen peroxide decay after 2 h at 1 and 2 bar, which corresponds with a moment when there is no

more clofibric acid (see Fig. 2b) and the amount of intermediates has been considerably reduced, remaining only carboxylic acids that are rather recalcitrant to be degraded by electro-Fenton treatment (Fig. 4b and c).

Considering that, it was found important to include an extra species in the model to improve the prediction of hydrogen peroxide behavior in the electro-Fenton reaction system. That species will be a scavenger, that might actually account for several compounds with a scavenging effect, and that could be generated anodically or cathodically. Thus, its generation is modelled as proportional to the current intensity as shown in Eqs. (18) and (19). At the same time, it was necessary to include the consumption caused by scavengers in the hydrogen peroxide balance giving rise to Eqs. (20) and (21) that improve, respectively, the Eqs. (8) and (10) previously proposed (the term that represented the abatement of hydrogen peroxide caused by clofibric acid has been eliminated in the improved equations, considering that they do not react directly).

$$V \cdot \frac{dC_{sc}}{dt} = \frac{I}{n_{sc} \cdot F} - k_{sc} \cdot C_{sc} \cdot C_{H_2O_2} \cdot V \tag{18}$$

$$C_{sc_{t+1}} = C_{sc_t} + \frac{\Delta t}{V} \cdot \left(\frac{I \cdot 60}{n_{sc} \cdot F} - k_{sc} \cdot C_{sc_t} \cdot C_{H_2O_{2_t}} \cdot V \right) \tag{19}$$

$$V \cdot \frac{dC_{H_2O_2}}{dt} = \frac{I}{n_{H_2O_2} \cdot F} \cdot \eta - k_d \cdot C_{H_2O_2} \cdot V - k_{Fen} \cdot C_{Fe} \cdot C_{H_2O_2} \cdot V - k_{sc} \cdot C_{sc_t} \cdot C_{H_2O_{2_t}} \cdot V \tag{20}$$

$$C_{H_2O_{2_{t+1}}} = C_{H_2O_{2_t}} + \frac{\Delta t}{V} \cdot \left(\frac{I \cdot 60}{n_{H_2O_2} \cdot F} \cdot \eta_t - k_d \cdot C_{H_2O_{2_t}} \cdot V - k_{Fen} \cdot C_{Fe} \cdot C_{H_2O_{2_t}} \cdot V - k_{sc} \cdot C_{sc_t} \cdot C_{H_2O_{2_t}} \cdot V \right) \tag{21}$$

Finally, the improved model was applied to the electro-Fenton treatment. The fitting of the estimation to the experimental data is shown in Fig. 7 and the fitting parameters in Table 5. It should be noted that, although the catalyst dosage is a known parameter of the electro-Fenton

assays, given that heterogeneous catalysis was used it is not clear to what extent the iron contained in the alginate beads is available for the Fenton reaction. Hence, the iron concentration (C_{Fe}) in Eq. (20) was used as a fitting parameter. For hydrogen peroxide, the estimations for the model with (dashed line) and without (solid line) considering the scavenger are presented in the graph. As observed, the model that takes into account the presence of scavengers of hydrogen peroxide fits better the trend of the experimental data (Fig. 7a). Additionally, the clofibric acid decay is accurately fitted (Fig. 7b). It is important to highlight that, as mentioned before, k_{CA} represents a pseudo-first order rate constant, which includes the concentration of hydroxyl radicals at the steady-state. Since at different pressures different amounts of hydrogen peroxide are generated, it is expected for the concentration of hydroxyl radicals to vary with pressure. As a consequence, the fitting parameter k_{CA} needs to be dependent with pressure (Table 5). Taking into consideration the fits obtained, it can be concluded that the model, defined with only a set of few fitting parameters, successfully represents the results obtained experimentally, hence validating the assumptions made and helping to understand the mechanisms behind the treatments applied.

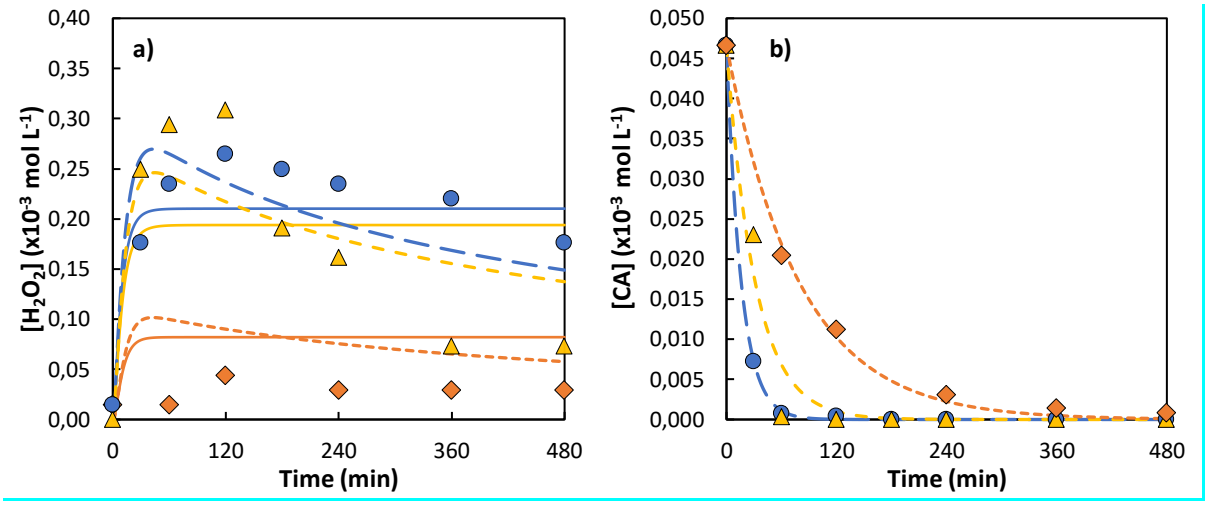

Fig. 7. Estimated concentration vs. experimental data of hydrogen peroxide concentration (a) and clofibric acid (CA) (b) during electro-Fenton at 0.25 A. Input data for the model: Δt = 1 min; V = 2.7 L; I = 0.25 A; $n_{H_2O_2}$ = 2; F = 96485 C mol^{-1} e^{-}; k_d = 0.0215 (for 0 bar), 0.0053

(for 1 bar), 0.0023 (for 2 bar) min^{-1}; k_{Fen} = 63 M^{-1} s^{-1} = 3780 M^{-1} min^{-1}; k_m = $6.84 \cdot 10^{-4}$ m s^{-1}; A = $4.95 \cdot 10^{-3}$ m^2; k = $1.52 \cdot 10^{-4}$ mol O_2 L^{-1}; $C_{O_2 sat}$ = $2.73 \cdot 10^{-4}$ (for 0 bar), $1.56 \cdot 10^{-3}$ (for 1 bar) and $2.84 \cdot 10^{-3}$ (for 2 bar) mol L^{-1}; n_{CA} = 1. Solid lines in (a) are model estimation without scavengers. Symbols are experimental data and dashed lines are estimations at 0 (◆, ----), 1 (▲, – – –) and 2 (●, — —) bar of gauge pressure.

Table 5. Fitting parameters of the model of electro-Fenton treatment considering the presence of scavengers.

Fitting parameter	Value obtained at		
	0 bar	1 bar	2 bar
k_{CA} (min^{-1})	0.0125	0.0315	0.0605
C_{lim} $(mol\ L^{-1})$	6.1		
C_{Fe} $(mol\ L^{-1})$	$2.3 \cdot 10^{-5}$		
n_{sc} $(mol\ e^-\ mol\ sc^{-1})$	1		
k_{sc} $(L\ min^{-1}\ mol^{-1})$	3.9		

Conclusions

From this research, the following conclusions can be drawn:

- The pressurized jet aerator has demonstrated to enhance hydrogen peroxide electrogeneration as pressure rises.
- Working above atmospheric pressure accelerates the heterogeneous electro-Fenton treatment of clofibric acid. However, not significant improvement is observed when increasing pressure from 1 to 2 bar.
- The pressurized system allows to operate at higher current intensities without reducing the efficiency of the specific charge usage.

- The specific energy consumption of the electrochemical cell for both hydrogen peroxide generation and clofibric acid abatement is considerably reduced when working under pressure.
- A pressure up to 2 bar proved not to damage the catalyst (iron-containing alginate beads) compared to atmospheric operation, and leaching was not increased with pressure.
- A mathematical model was obtained that faithfully represents the behavior of the reaction system for the electrogeneration of hydrogen peroxide and the abatement of clofibric acid.
- The model has shown that the hydrogen peroxide decomposition rate in hydrogen peroxide generation assays is inversely related to pressure, and that it is necessary to consider the presence of scavenging species to model hydrogen peroxide behavior in electro-Fenton assays above atmospheric pressure.

Acknowledgments

This research has been financially supported by the Spanish Ministry of Science, Innovation and Universities by means of the contract of the PhD student Verónica Poza Nogueiras (FPU16/02644), the E3TECH Network of Excellence (CTQ2017-90659-REDT) and the Projects CTM2017-87326-R and PID2019-110904RB-I00. Financial support from Junta de Comunidades de Castilla-La Mancha (JCCM) through the project SBPLY/17/180501/000396 is also gratefully acknowledged. Furthermore, authors would like to acknowledge the University of Vigo for funding the mobility action of Verónica Poza Nogueiras at the University of Castilla-La Mancha.

References

[1] A. Klančar, J. Trontelj, A. Kristl, A. Meglič, T. Rozina, M.Z. Justin, et al., An advanced oxidation process for wastewater treatment to reduce the ecological burden from pharmacotherapy and the agricultural use of pesticides, Ecol. Eng. 97 (2016) 186-195.

[2] H. Lin, X. Tang, J. Wang, Q. Zeng, H. Chen, W. Ren, et al., Enhanced visible-light photocatalysis of clofibric acid using graphitic carbon nitride modified by cerium oxide nanoparticles, J. Hazard. Mater. (2020) 124204.

[3] J.P. Emblidge, M.E. DeLorenzo, Preliminary risk assessment of the lipid-regulating pharmaceutical clofibric acid, for three estuarine species, Environ. Res. 100 (2006) 216-226.

[4] K. Zhu, X. Wang, M. Geng, D. Chen, H. Lin, H. Zhang, Catalytic oxidation of clofibric acid by peroxydisulfate activated with wood-based biochar: Effect of biochar pyrolysis temperature, performance and mechanism, Chem. Eng. J. 374 (2019) 1253-1263.

[5] H. Buser, M.D. Müller, N. Theobald, Occurrence of the pharmaceutical drug clofibric acid and the herbicide mecoprop in various Swiss lakes and in the North Sea, Environ. Sci. Technol. 32 (1998) 188-192.

[6] M. Stumpf, T.A. Ternes, R. Wilken, Silvana Vianna Rodrigues, W. Baumann, Polar drug residues in sewage and natural waters in the state of Rio de Janeiro, Brazil, Sci. Total Environ. 225 (1999) 135-141.

[7] M. Kuster, M.J. López de Alda, M.D. Hernando, M. Petrovic, J. Martín-Alonso, D. Barceló, Analysis and occurrence of pharmaceuticals, estrogens, progestogens and polar pesticides in sewage treatment plant effluents, river water and drinking water in the Llobregat river basin (Barcelona, Spain), J. Hydrol. 358 (2008) 112-123.

[8] S. Díaz-Cruz, D. Barceló, Occurrence and Analysis of Selected Pharmaceuticals and Metabolites as Contaminants Present in Waste Waters, Sludge and Sediments, Handb. Environ. Chem. 5 (2004) 227-260.

[9] M.M. Bello, A.A. Abdul Raman, A. Asghar, A review on approaches for addressing the limitations of Fenton oxidation for recalcitrant wastewater treatment, Process Saf. Environ. Prot. 126 (2019) 119-140.

[10] C.M. Domínguez, N. Oturan, A. Romero, A. Santos, M.A. Oturan, Optimization of electro-Fenton process for effective degradation of organochlorine pesticide lindane, Catal. Today 313 (2018) 196-202.

[11] S. Rezgui, A. Amrane, F. Fourcade, A. Assadi, L. Monser, N. Adhoum, Electro-Fenton catalyzed with magnetic chitosan beads for the removal of Chlordimeform insecticide, Appl. Catal. B: Environ. 226 (2018) 346-359.

[12] J. Meijide, P.S.M. Dunlop, M. Pazos, M.A. Sanromán, Heterogeneous electro-fenton as "Green" technology for pharmaceutical removal: A review, Catalysts 11 (2021) 1-22.

[13] I. Sirés, E. Brillas, Upgrading and expanding the electro-Fenton and related processes, Curr. Opin. Electrochem. 27 (2021) 100686.

[14] J.F. Pérez, J. Llanos, C. Sáez, C. López, P. Cañizares, M.A. Rodrigo, On the design of a jet-aerated microfluidic flow-through reactor for wastewater treatment by electro-Fenton, Sep. Purif. Technol. 208 (2019) 123-129.

[15] J.F. Pérez, J. Llanos, C. Sáez, C. López, P. Cañizares, M.A. Rodrigo, The pressurized jet aerator: A new aeration system for high-performance H_2O_2 electrolyzers, Electrochem. Commun. 89 (2018) 19-22.

[16] W. Zhou, X. Meng, J. Gao, A.N. Alshawabkeh, Hydrogen peroxide generation from O_2 electroreduction for environmental remediation: A state-of-the-art review, Chemosphere 225 (2019) 588-607.

[17] J.F. Pérez, A. Galia, M.A. Rodrigo, J. Llanos, S. Sabatino, C. Sáez, et al., Effect of pressure on the electrochemical generation of hydrogen peroxide in undivided cells on carbon felt electrodes, Electrochim. Acta 248 (2017) 169-177.

[18] O. Scialdone, A. Galia, C. Gattuso, S. Sabatino, B. Schiavo, Effect of air pressure on the electro-generation of H_2O_2 and the abatement of organic pollutants in water by electro-Fenton process, Electrochim. Acta 182 (2015) 775-780.

[19] J.F. Pérez, J. Llanos, C. Sáez, C. López, P. Cañizares, M.A. Rodrigo, The jet aerator as oxygen supplier for the electrochemical generation of H_2O_2, Electrochim. Acta 246 (2017) 466-474.

[20] J.F. Pérez, J. Llanos, C. Sáez, C. López, P. Cañizares, M.A. Rodrigo, Towards the scale up of a pressurized-jet microfluidic flow-through reactor for cost-effective electro-generation of H_2O_2, J. Clean. Prod. 211 (2019) 1259-1267.

[21] V. Poza-Nogueiras, Á Moratalla, M. Pazos, Á Sanromán, C. Sáez, M.A. Rodrigo, Towards a more realistic heterogeneous electro-Fenton, J Electroanal Chem (2021) 115475.

[22] A.H. Ltaïef, S. Sabatino, F. Proietto, S. Ammar, A. Gadri, A. Galia, et al., Electrochemical treatment of aqueous solutions of organic pollutants by electro-Fenton with natural heterogeneous catalysts under pressure using Ti/IrO_2-Ta_2O_5 or BDD anodes, Chemosphere 202 (2018) 111-118.

[23] N. Hamdi, F. Proietto, H. Ben Amor, A. Galia, R. Inguanta, S. Ammar, et al., Effective Removal and Mineralization of 8-Hydroxyquinoline-5-sulfonic Acid through a Pressurized Electro-Fenton-like Process with Ni−Cu−Al Layered Double Hydroxide, ChemElectroChem 7 (2020) 2457-2465.

[24] J.F. Pérez, J. Llanos, C. Sáez, C. López, P. Cañizares, M.A. Rodrigo, Development of an innovative approach for low-impact wastewater treatment: A microfluidic flow-through electrochemical reactor, Chem. Eng. J. 351 (2018) 766-772.

[25] O. Iglesias, J. Gómez, M. Pazos, M.Á Sanromán, Electro-Fenton oxidation of imidacloprid by Fe alginate gel beads, Appl. Catal. B Environ. 144 (2014) 416-424.

[26] G.M. Eisenberg, Colorimetric Determination of Hydrogen Peroxide, Ind. Eng. Chem. Anal. Ed. 15 (1943) 327-328.

[27] M. Geng, Z. Duan, Prediction of oxygen solubility in pure water and brines up to high temperatures and pressures, Geochim. Cosmochim. Acta 74 (2010) 5631-5640.

[28] G.A. Kolyagin, V.L. Kornienko, Pilot laboratory electrolyzer for electrosynthesis of hydrogen peroxide in acid and alkaline solutions, Russ. J. Appl. Chem. 84 (2011) 68-71.

[29] W.R.P. Barros, T. Ereno, A.C. Tavares, M.R.V. Lanza, In Situ Electrochemical Generation of Hydrogen Peroxide in Alkaline Aqueous Solution by using an Unmodified Gas Diffusion Electrode, ChemElectroChem 2 (2015) 714-719.

[30] Z. Chen, H. Dong, H. Yu, H. Yu, In-situ electrochemical flue gas desulfurization via carbon black-based gas diffusion electrodes: Performance, kinetics and mechanism, Chem. Eng. J. 307 (2017) 553-561.

[31] X. Yu, M. Zhou, G. Ren, L. Ma, A novel dual gas diffusion electrodes system for efficient hydrogen peroxide generation used in electro-Fenton, Chem. Eng. J. 263 (2015) 92-100.

[32] M. Zarei, D. Salari, A. Niaei, A. Khataee, Peroxi-coagulation degradation of C.I. Basic Yellow 2 based on carbon-PTFE and carbon nanotube-PTFE electrodes as cathode, Electrochim. Acta 54 (2009) 6651-6660.

[33] G.D.O.S. Santos, K.I.B. Eguiluz, G.R. Salazar-Banda, C. Sáez, M.A. Rodrigo, Testing the role of electrode materials on the electro-Fenton and photoelectro-Fenton degradation of clopyralid, J. Electroanal. Chem. 871 (2020) 114291.

[34] E. Petrucci, A. Da Pozzo, L. Di Palma, On the ability to electrogenerate hydrogen peroxide and to regenerate ferrous ions of three selected carbon-based cathodes for electro-Fenton processes, Chem. Eng. J. 283 (2016) 750-758.

[35] A.D. Marincean, S.A. Dorneanu, P. Ilea, Hydrogen peroxide electrosynthesis using recycled graphite granules as 3D cathode. Comparison with other commercial materials and optimization studies, Rev. Chim. 71 (2020) 102-115.

[36] C.A. Martínez-Huitle, M.A. Rodrigo, I. Sirés, O. Scialdone, Single and Coupled Electrochemical Processes and Reactors for the Abatement of Organic Water Pollutants: A Critical Review, Chem. Rev. 115 (2015) 13362-13407.

[37] W. Zhou, X. Meng, J. Gao, F. Sun, G. Zhao, Janus graphite felt cathode dramatically enhance the H_2O_2 yield from O_2 electroreduction by the hydrophilicity-hydrophobicity regulation, Chemosphere 278 (2021) 130382.

[38] J. Zhang, S. Qiu, H. Feng, T. Hu, Y. Wu, T. Luo, et al., Efficient degradation of tetracycline using core–shell Fe@Fe_2O_3-CeO_2 composite as novel heterogeneous electro-Fenton catalyst, Chem. Eng. J. 428 (2022) 131403.

[39] E. Brillas, I. Sirés, M.A. Oturan, Electro-fenton process and related electrochemical technologies based on Fenton's reaction chemistry, Chem. Rev. 109 (2009) 6570-6631.

[40] P. Cañizares, J. García-Gómez, I. Fernández de Marcos, M.A. Rodrigo, J. Lobato, Measurement of mass-transfer coefficients by an electrochemical technique, J. Chem. Educ. 83 (2006) 1204-1207.

[41] Z. Qiang, J. Chang, C. Huang, Electrochemical generation of hydrogen peroxide from dissolved oxygen in acidic solutions, Water Res. 36 (2002) 85-94.

[42] J. Bacardit, I. Oller, M.I. Maldonado, E. Chamarro, S. Malato, S. Esplugas, Simple models for the control of photo-fenton by monitoring H_2O_2, J. Adv. Oxid. Technol. 10 (2007) 219-228.

[43] S. Ahmadzadeh, M. Dolatabadi, Removal of acetaminophen from hospital wastewater using electro-Fenton process, Environ. Earth Sci. 77 (2018) 53.

[44] P. Dong, W. Liu, S. Wang, H. Wang, Y. Wang, C. Zhao, In suit synthesis of Fe_3O_4 on carbon fiber paper@polyaniline substrate as novel self-supported electrode for heterogeneous electro-Fenton oxidation, Electrochim. Acta 308 (2019) 54-63.

[45] M. Dolatabadi, M.T. Ghaneian, C. Wang, S. Ahmadzadeh, Electro-Fenton approach for highly efficient degradation of the herbicide 2,4-dichlorophenoxyacetic acid from agricultural wastewater: Process optimization, kinetic and mechanism, J. Mol. Liq. 334 (2021) 116116.

[46] F.E. Titchou, H. Zazou, H. Afanga, J.E. Gaayda, R. Ait Akbour, M. Hamdani, et al., Electro-Fenton process for the removal of Direct Red 23 using BDD anode in chloride and sulfate media, J. Electroanal. Chem. 897 (2021) 115560.

[47] F.E. Titchou, H. Zazou, H. Afanga, J.E. Gaayda, R. Ait Akbour, P.V. Nidheesh, et al., An overview on the elimination of organic contaminants from aqueous systems using electrochemical advanced oxidation processes, J. Water Process. Eng. 41 (2021) 102040.

[48] M. Rodríguez-Peña, J.A. Barrios Pérez, J. Llanos, C. Saez, C.E. Barrera-Díaz, M.A. Rodrigo, Electrochemical generation of ozone using a PEM electrolyzer at acidic pHs, Sep. Purif. Technol. 267 (2021) 118672.